Localization of Cyclopropane Modifications in Bacterial Lipids via 213 nm Ultraviolet Photodissociation Mass Spectrometry

Molly S. Blevins, Dustin R. Klein, and Jennifer S. Brodbelt*

Department of Chemistry, University of Texas at Austin, Austin, TX 78712, United States

*Corresponding author: jbrodbelt@cm.utexas.edu

Supporting Information

Table of Contents

Content	Page no.
1. Possible fragmentation pathway for UVPD of cyclopropane rings in bacterial lipids	S-2
2. *In vivo* generation of bacterial cyclopropane glycerophospholipid from double bond precursor	S-3
3. Structures of all cyclopropane lipid standards	S-4
4. MS1 spectra of PE (16:0/17:1(c9Z)) and PC (16:0/17:1(c9Z)) with corresponding structures	S-5
5. Calibration curve for PE (16:0/17:1(c9Z)) cyclopropane diagnostic ion LC/UVPD-MS peak areas as a function of injection amount	S-6
6. HCD spectrum of α-MA (C-80(c16Z, c32Z)) with fragment ion map	S-7
7. Comparison of 193 and 213 nm UVPD for cyclopropane localization in PE (16:0/17:1(c9Z))	S-8
8. HCD and UVPD spectra of methoxy-MA of *m/z* 1224 with corresponding fragment ion maps	S-9
9. LC-MS base peak chromatogram of *Mtb* H37rV lipid extract	S-10
10. LC-MS base peak chromatograms of *Mtb* HN878 and CDC1551 lipid extracts with corresponding lists of identified MAs	S-11

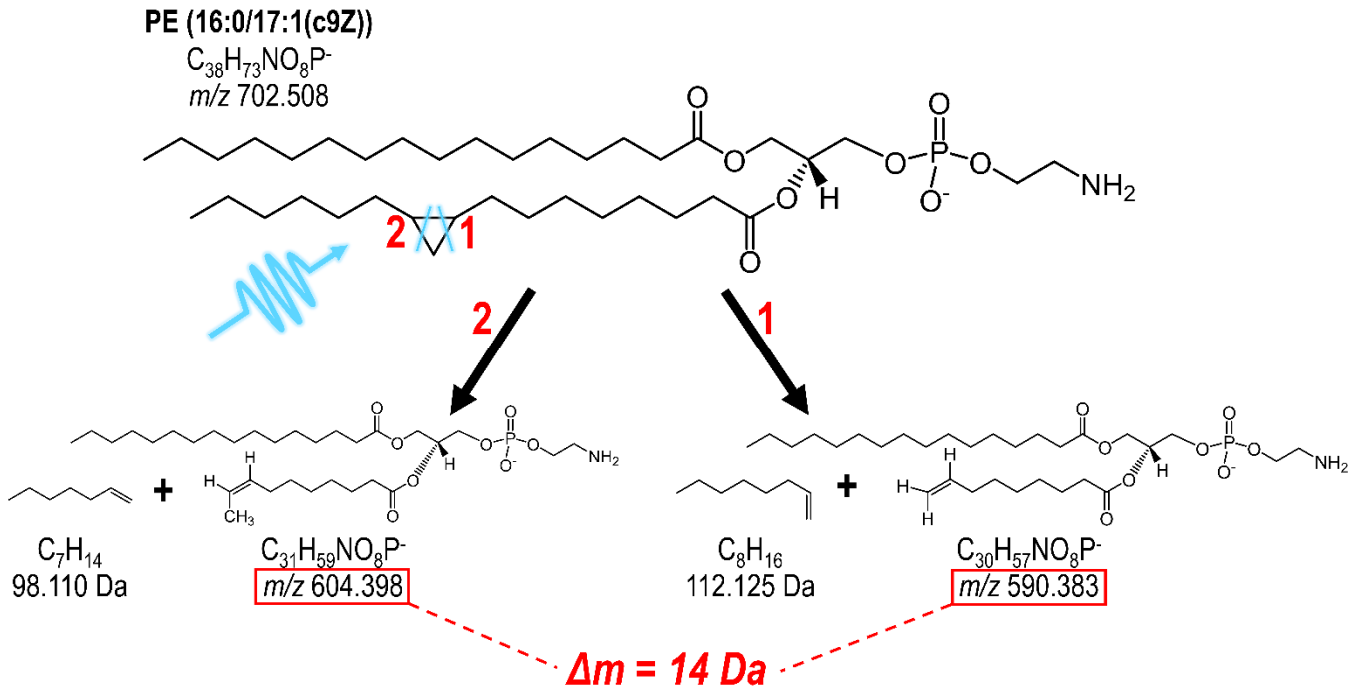

Scheme S1. Possible fragmentation pathway for UVPD of cyclopropane rings in bacterial lipids with example shown for PE (16:0/17:1(c9Z)). Boxed products will be detected via MS as depicted product ions retains the phospholipid headgroup, differing by CH_2 and accounting for an observed mass difference of 14 Da

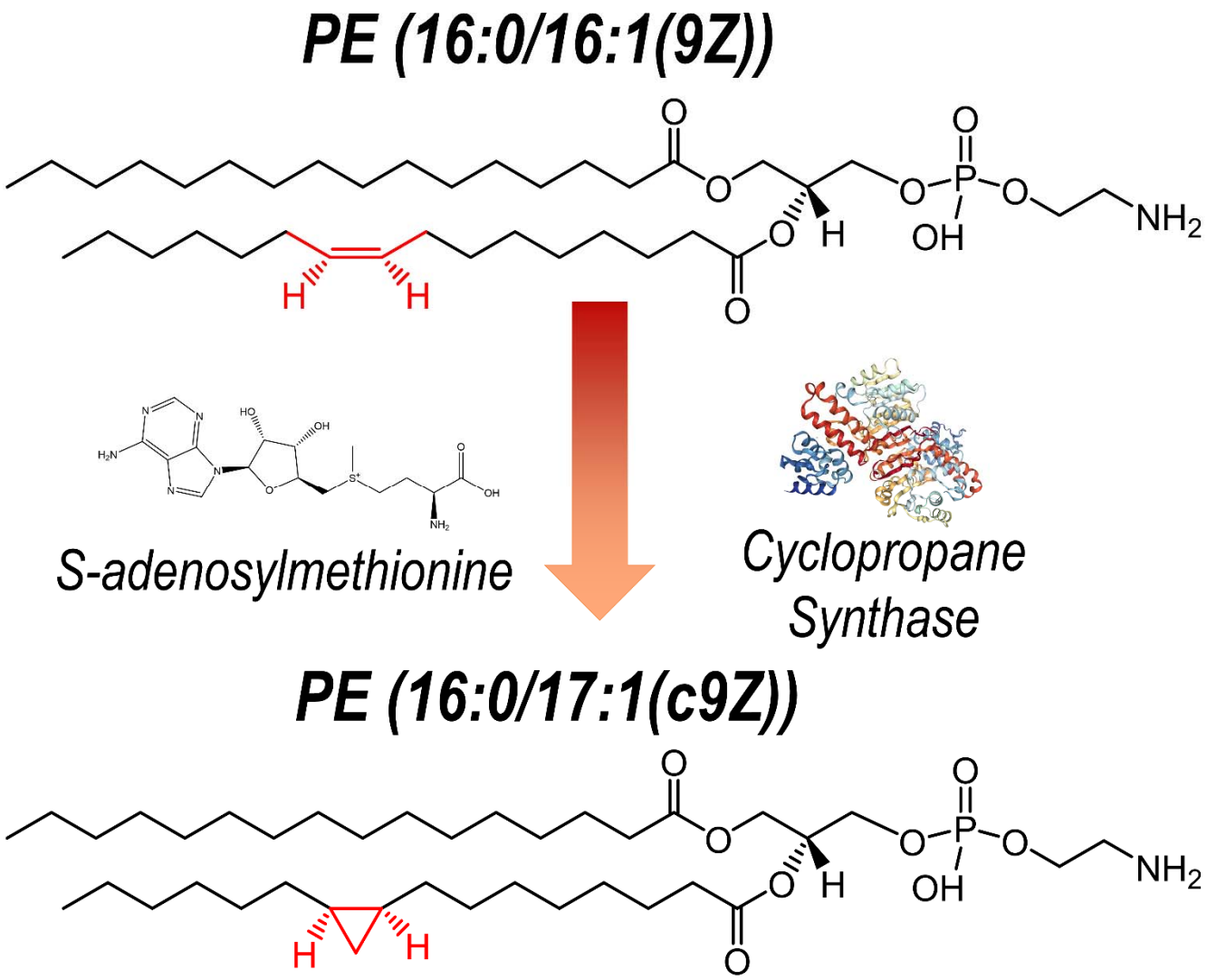

Scheme S2. *In vivo* generation of bacterial cyclopropane glycerophospholipid from double bond precursor via S-adenosylmethionine methylene addition and cyclopropane synthase catalysis (PDB entry 6BQC)

Lipid Name	Lipid Structure	Exact Mass (Da)
(2R)-3-(((2-aminoethoxy)(hydroxy)phosphoryl)oxy)-2-((8-((1S,2R)-2-hexylcyclopropyl)octanoyl)oxy)propyl palmitate **PE (16:0/17:1(c9Z))**	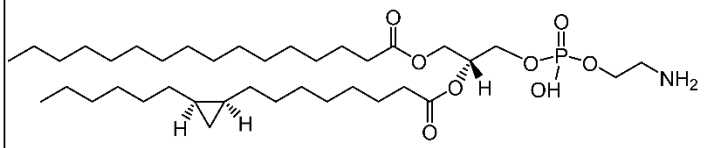	**703.515**
2-((((R)-2-((8-((1S,2R)-2-hexylcyclopropyl)octanoyl)oxy)-3-(palmitoyloxy)propoxy)(hydroxy)phosphoryl)oxy)-N,N,N-trimethylethan-1-aminium **PC (16:0/17:1(c9Z))**	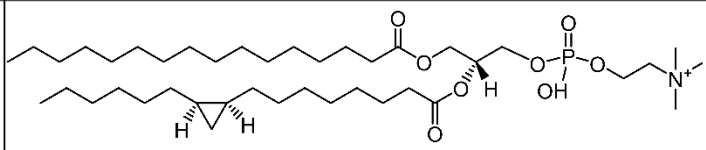	**746.569**
(2R)-2-((1R)-1-hydroxy-14-(2-(14-(2-octadecylcyclopropyl)tetradecyl)cyclopropyl)tetradecyl)hexacosa-3,5,7,9,11,13,15,17,19,21,23,25-dodecaynoic acid compound with dihydrogen (1:24) **α-mycolic acid (C-80(c16Z, c32Z))**	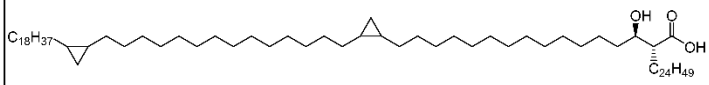	**1137.174**

Table S1. Structures of all cyclopropane lipid standards

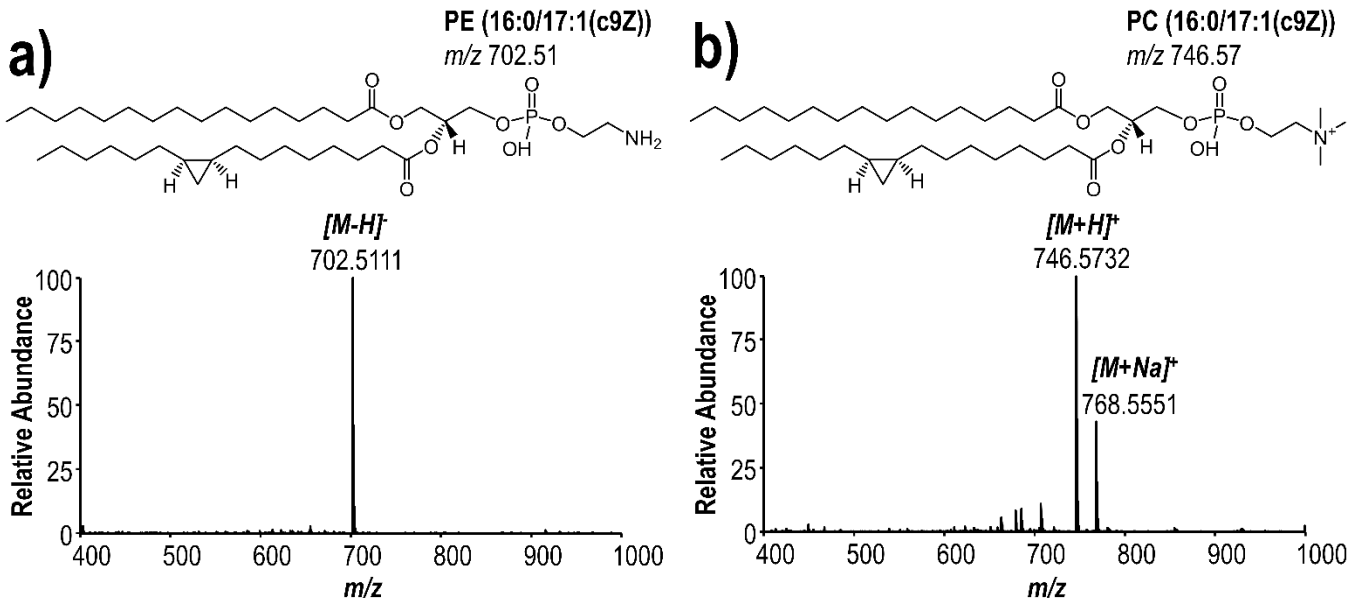

Figure S1. MS1 spectra of **a)** PE (16:0/17:1(c9Z)) in negative ion mode and **b)** PC (16:0/17:1(c9Z)) in positive ion mode with corresponding structures.

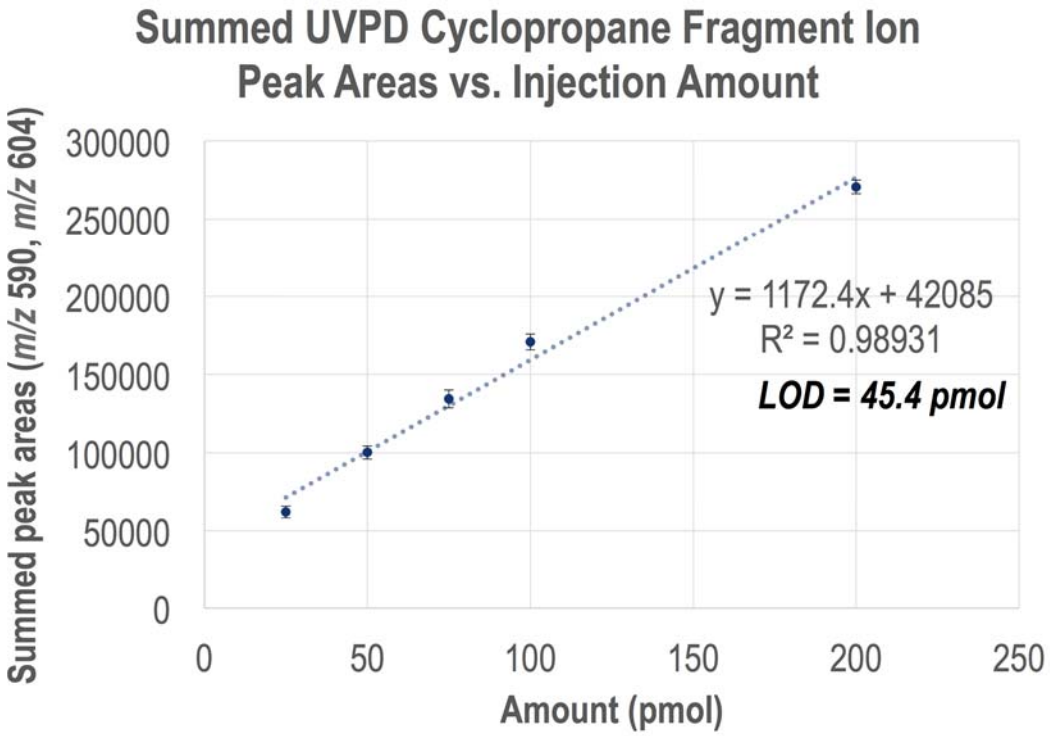

Figure S2. Calibration curve for PE (16:0/17:1(c9Z)) based on detection of diagnostic ions (m/z 590 and 604) from negative ion mode 213 nm LC/UVPD-MS enabling determination of LOD as 45 pmol. Calibration curve was generated based on linear regression analysis of peak areas with seven-point boxcar smoothing over the range of 20 to 200 pmol with S/N=3 and LOD experiments were performed using an activation period of 100 msec (corresponding to 250 pulses) and performed in triplicate as indicated by error bars included on the graph. For this LOD measurement, the UVPD efficiency of caffeine used to calibrate and optimize UVPD performance was measured as 25% using 125 laser pulses (50 ms activation period).

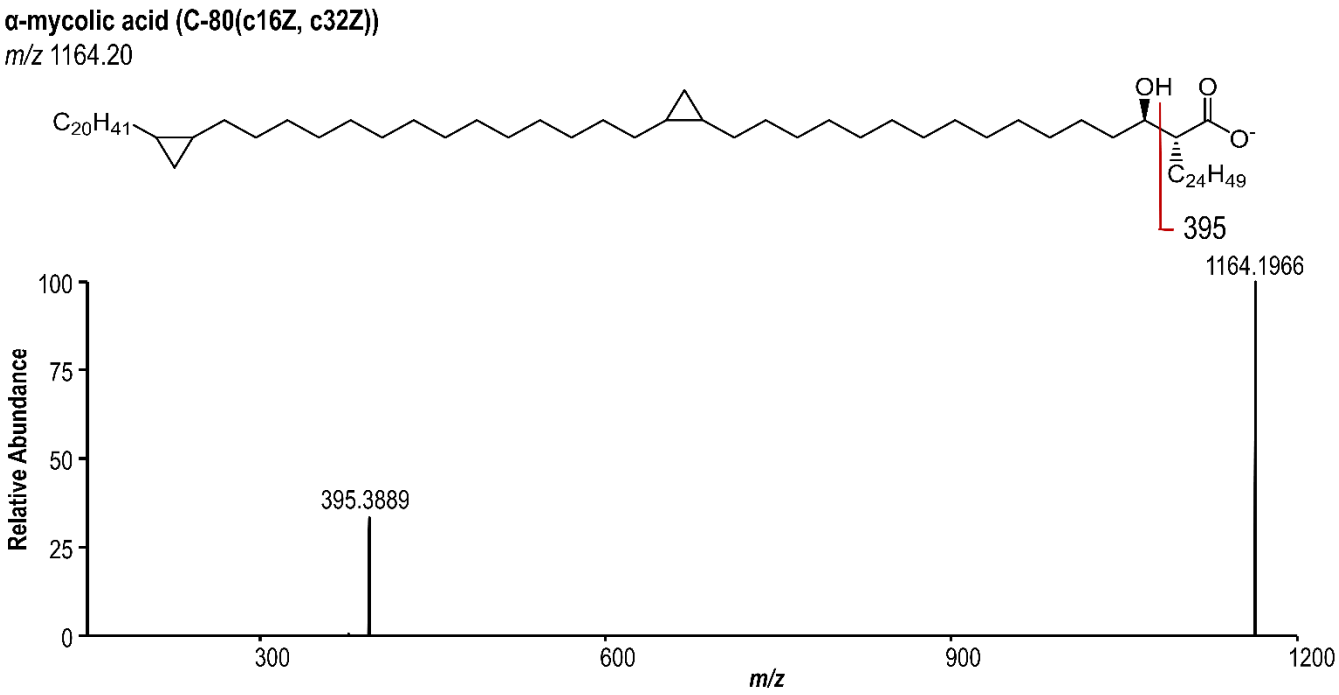

Figure S3. Negative mode HCD spectrum of α-mycolic acid (C-80(c16Z, c32Z)) with corresponding fragment ion map.

a)

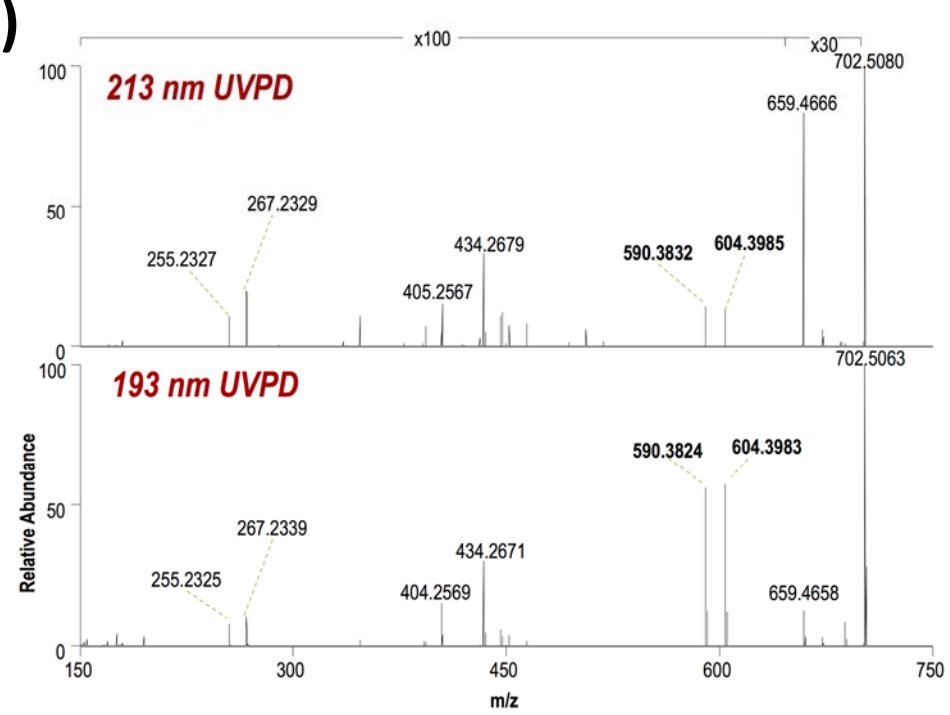

b)

Wavelength (nm)	213	193
Activation parameters	500 pulses 1.5 uJ per pulse 200 ms activation period	10 pulses 5 mJ per pulse 20 ms activation period
Abundance of precursor prior to UVPD (m/z 702.5)	111,093,064	29,162,016
Summed abundances of diagnostic ions (m/z 590 and 604)	167,758	318,411
Fragmentation efficiency (%) (fragment abundance/precursor abundance)	0.2	1.1

Figure S4. a) Comparison of negative mode 193 and 213 nm UVPD spectra of PE (16:0/17:1(c9Z)) of precursor *m/z* 702 with cyclopropane diagnostic ions of *m/z* 590 and *m/z* 604 labelled in bold font. The 100X magnification applies to both spectra. **b)** Summary of 193 and 213 nm UVPD parameters along with fragment-to-precursor ratio showing higher efficiency of 193 nm UVPD compared to 213 nm UVPD. For each type of UVPD, the laser is unfocused.

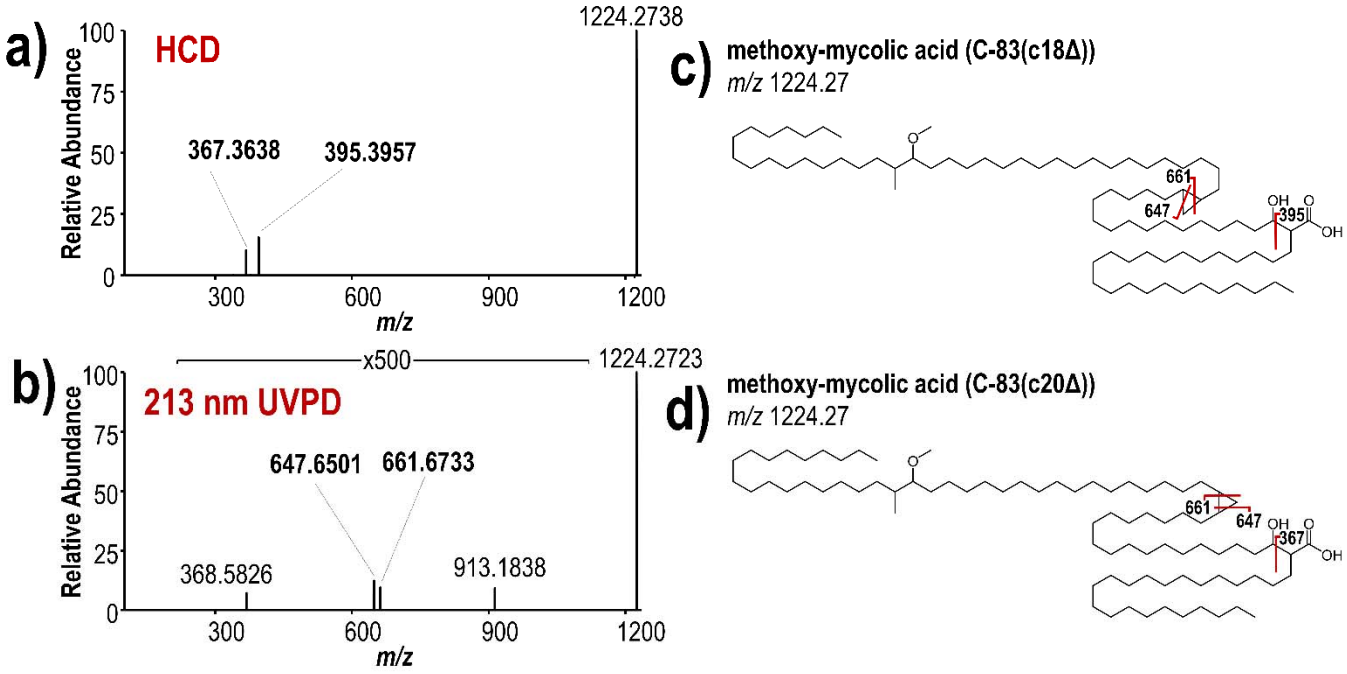

Figure S5. a) HCD and **b)** 213 nm UVPD spectra of methoxy-mycolic acid of *m/z* 1224 in negative ion mode and corresponding structural identifications with fragment maps: **c)** methoxy-mycolic acid (C-83(c18Δ)) and **d)** methoxy-mycolic acid (C-83(c20Δ)).

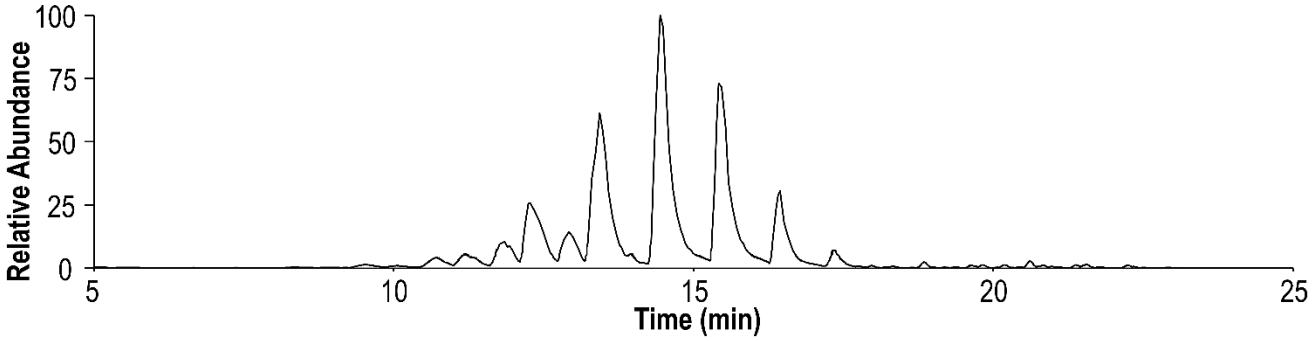

Figure S6. Negative mode LC-MS base peak chromatogram of *Mtb* H37rV lipid extract.

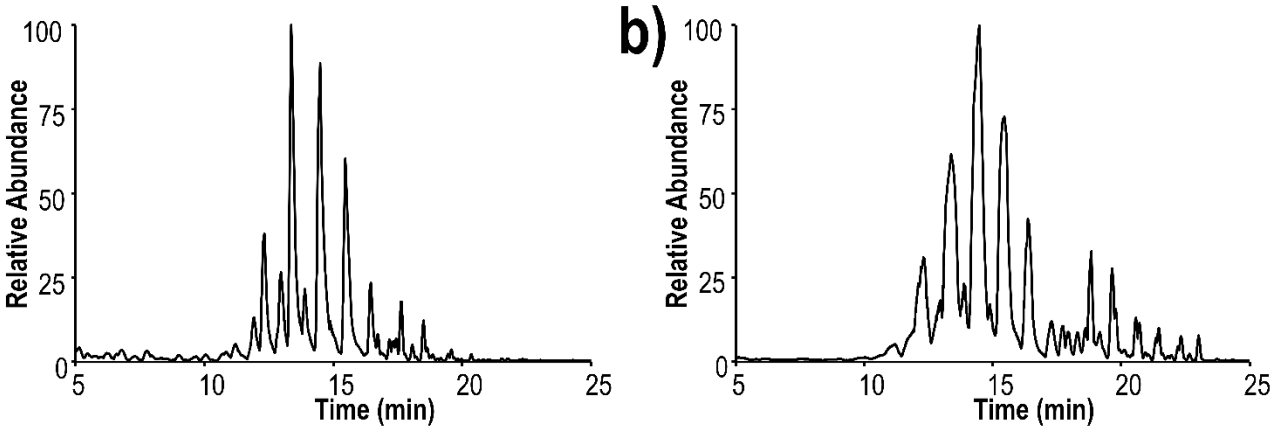

c)

m/z [M-H]⁻	Chemical Formula	MA Class	m/z R_2 (α branch)	C_{distal} m/z diagnostic ions		C_{distal} Ring position	$C_{proximal}$ m/z diagnostic ions		$C_{proximal}$ Ring position
1108.1515	$C_{76}H_{148}O_3$	alpha	367, 395	563.5511	577.5593	c12Δ (395), c14Δ (367)	799.8073	813.8130	c28Δ (395), c30Δ (367)
							813.8130	827.8345	c29Δ (395), c31Δ (367)
							827.8345	841.8480	c30Δ (395), c32Δ (367)
1136.1825	$C_{78}H_{152}O_3$	alpha	367, 395	591.5862	605.5973	c14Δ (395), c16Δ (367)	827.8371	841.8550	c30Δ (395), c32Δ (367)
							841.8550	855.8824	c31Δ (395), c33Δ (367)
							855.8824	869.8666	c32Δ (395), c34Δ (367)
1164.2151	$C_{80}H_{156}O_3$	alpha	367, 395	619.6111	633.6366	c16Δ (395), c18Δ (367)	855.8658	869.8855	c30Δ (395), c32Δ (367)
1224.2725	$C_{83}H_{164}O_3$	methoxy	367, 395	647.6436	661.6670	c18Δ (395), c20Δ (367)	-	-	-
1252.3030	$C_{85}H_{168}O_4$	methoxy	395	675.6806	689.7073	c20Δ	-	-	-
1278.3196	$C_{87}H_{172}O_4$	keto	395	661.6498	675.6744	c19Δ	-	-	-
1280.3351	$C_{87}H_{172}O_4$	methoxy	395	675.6864	689.7028	c20Δ	-	-	-
				689.7028	703.6973	c21Δ	-	-	-
				703.6973	717.7114	c22Δ	-	-	-
1294.3502	$C_{86}H_{174}O_4$	methoxy	395	661.6572	675.6744	c19Δ	-	-	-

d)

m/z [M-H]⁻	Chemical Formula	MA Class	m/z R_2 (α branch)	C_{distal} m/zdiagnostic ions		C_{distal} Ring position	$C_{proximal}$ m/zdiagnostic ions		$C_{proximal}$ Ring position
1108.1520	$C_{76}H_{148}O_3$	alpha	339, 367, 395	563.5494	577.5612	c12Δ (395), c14Δ (367), c16Δ (339)	799.8046	813.8129	c28Δ (395), c30Δ (367), c32Δ (339)
							813.8129	827.8302	c29Δ (395), c31Δ (367), c33Δ (339)
							827.8302	841.8393	c30Δ (395), c32Δ (367), c34Δ (339)
1136.1833	$C_{78}H_{152}O_3$	alpha	367, 395	591.5839	605.6035	c14Δ (395), c16Δ (367)	827.8284	841.8535	c30Δ (395), c32Δ (367)
							841.8535	855.8817	c31Δ (395), c33Δ (367)
1164.2148	$C_{80}H_{156}O_3$	alpha	367, 395	619.6184	633.6296	c16Δ (395), c18Δ (367)	855.8654	869.8852	c30Δ (395), c32Δ (367)
							869.8852	883.9082	c31Δ (395), c33Δ (367)
1224.2728	$C_{83}H_{164}O_3$	methoxy	367, 395	647.6470	661.6630	c18Δ (395), c20Δ (367)	-	-	-
1252.3030	$C_{85}H_{168}O_4$	methoxy	367, 395	661.6651	675.6806	c19Δ (395), c21Δ (367)	-	-	-
				675.6806	689.6962	c20Δ (395), c22Δ (367)	-	-	-
1280.3350	$C_{87}H_{172}O_4$	methoxy	367, 395	675.6934	689.6998	c20Δ (395), c22Δ (367)	-	-	-
				689.6998	703.7048	c21Δ (395), c23Δ (367)	-	-	-
				703.7048	717.7048	c22Δ (395), c24Δ (367)	-	-	-
1294.3500	$C_{86}H_{174}O_4$	methoxy	367, 395	661.6513	675.6749	c19Δ (395), c21Δ (367)	-	-	-
1308.3669	$C_{88}H_{176}O_4$	methoxy	395	703.7062	717.7184	c22Δ	-	-	-
1322.3833	$C_{90}H_{176}O_4$	methoxy	367, 395	689.6821	703.7161	c21Δ (395), c23Δ (367)			

Figure S7. Negative mode LC-MS base peak chromatogram for **a)** *Mtb* HN878 lipid extract and **b)** *Mtb* CDC1551 lipid extract, and list of identified mycolic acids from LC-MS/MS for **c)** *Mtb* HN878 lipid extract and **d)** *Mtb* CDC1551 lipid extract.